HHS Public Access

Author manuscript

Cell Rep. Author manuscript; available in PMC 2016 June 16.

Published in final edited form as:

Cell Rep. 2015 June 16; 11(10): 1651–1666. doi:10.1016/j.celrep.2015.05.013.

Fragile X Proteins FMRP and FXR2P control synaptic GluA1 expression and neuronal maturation via distinct mechanisms

Weixiang Guo[1,2], **Eric D. Polich**[2], **Juan Su**[2], **Yu Gao**[2], **Devin M. Christopher**[3], **Andrea M. Allan**[3], **Min Wang**[1], **Feifei Wang**[1], **Guangfu Wang**[4], and **Xinyu Zhao**[2]

[1]State Key Laboratory for Molecular and Developmental Biology, Institute of Genetics and Developmental Biology, Chinese Academy of Sciences, Beijing 100101, China

[2]Waisman Center and Department of Neuroscience, University of Wisconsin-Madison, Madison, WI 53705, USA

[3]Department of Neurosciences, University of New Mexico, Albuquerque, NM 87131, USA

[4]Department of Pharmacology, University of Virginia School of Medicine, Charlottesville, VA 22908, USA

Abstract

Fragile X mental retardation protein (FMRP) and its autosomal paralog FXR2P are selective neuronal RNA-binding proteins, and mice that lack either protein exhibit cognitive deficits. Although double-mutant mice display more severe learning deficits than single mutants, the molecular mechanism behind this remains unknown. In the present study, we discovered that FXR2P (also known as FXR2) is important for neuronal dendritic development. FMRP and FXR2P additively promote the maturation of new neurons by regulating a common target, the AMPA receptor GluA1, but they do so via distinct mechanisms: FXR2P binds and stabilizes *GluA1* mRNA and enhances subsequent protein expression, whereas FMRP promotes GluA1 membrane delivery. Our findings unveil important roles for FXR2P and GluA1 in neuronal development, uncover a regulatory mechanism of GluA1, and reveal a unique functional convergence between fragile X proteins in neuronal development.

Graphical Abstract

Corresponding author: Xinyu Zhao (Waisman Center and Department of Neuroscience, University of Wisconsin-Madison School of Medicine and Public Health, Madison, WI 53705, USA; Phone: (608) 263-9906; xzhao69@wisc.edu).

The authors declare no conflict of interest.

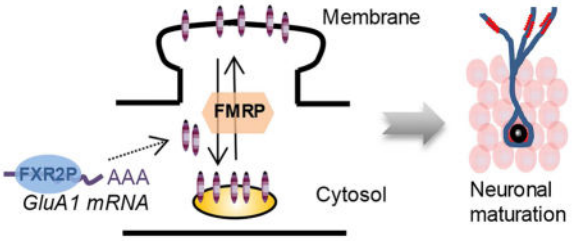

Introduction

The formation of an appropriate neural network is required for normal brain function. During development, neurons must develop the dendrites, spines, and axons that allow them to integrate into the neural circuitry. This maturation process is regulated by complex molecular mechanisms that are defective in many disorders, including autism and schizophrenia (Smrt and Zhao, 2010). Adult newborn neurons undergo a development process that recapitulates the early developmental one (Ge et al., 2007)and these regulatory mechanisms are highly conserved between embryonic and adult neurogenesis (Eisch and Petrik, 2012; Ming and Song, 2011). Understanding them may therefore uncover novel therapeutic targets.

Fragile X syndrome (FXS), the most common inherited intellectual disability and the largest single genetic contributor to autism is caused by a loss of function of the X-linked fragile X mental retardation protein (FMRP). (Hagerman and Polussa, 2015; Wang et al., 2012). Individuals with FXS display impaired cognition and learning. We have shown that FMRP-deficiency in adult neural stem cells leads to reduced neuronal production and maturation, resulting in neurogenesis-associated learning deficits (Guo et al., 2011a; Guo et al., 2012; Luo et al., 2010). In mammals, FMRP has two conserved autosomal paralogs, FXR1P and FXR2P (also known as FXR1 and FXR2). and all three RNA-binding proteins are enriched in neurons. They share similar functional domains, but diverge in the C-termini and in the nucleolar localization signal sequence, suggesting they possess both common and distinct functions (Darnell et al., 2009; Li and Zhao, 2014). Studies have shown that FXS proteins have the ability to interact with each other, and FMRP and FXR2P double knockout mice display more severe neurobehavioral abnormalities compared to single-mutant mice (Spencer et al., 2006). Nevertheless, the functional convergence among FXR proteins in neuronal development and underlying molecular mechanisms remain unclear.

FXR2P-deficient (*Fxr2 KO*) mice display changed gene expression in the brain, altered synaptic plasticity, and impaired learning (Cavallaro et al., 2008; Spencer et al., 2006; Zhang et al., 2009). FXR2P is at the center of an autism protein interactome network and interacts with more syndromic autism proteins than FMRP (Sakai et al., 2011). Moreover, FXR2P is present in more fragile X granules in the brain versus FMRP (Akins et al., 2012). We have demonstrated that FXR2P deficiency affects the fate of neural stem cells in the adult hippocampus (Guo et al., 2011b); however, the function of FXR2P in neuronal development remains unclear.

In the present study, we investigated the role of FXR2P in neuronal development and explored the potential functional interactions between FMRP and FXR2P. We discovered that FXR2P promotes the dendritic development of new neurons by directly targeting the AMPA receptor GluA1. FXR2P increased *GluA1* mRNA stability which directly impacts dendritic development.. In contrast, FMRP promoted membrane delivery of GluA1, without affecting total GluA1 protein levels. We discovered that FMRP and FXR2P double-deficient new neurons had significantly lower membrane GluA1 levels and more impaired neuronal maturation than single-mutant neurons. Therefore, FMRP and FXR2P regulate neuronal maturation through the same target, GluA1, but they do so via distinct mechanisms. Our findings unveil important roles for FXR2P and GluA1 in neuronal development, uncover a regulatory mechanism of GluA1, and reveal a unique functional convergence of fragile X proteins in neuronal development.

RESULTS

FXR2P Deficiency Impairs the Morphological Development and Connectivity of Adult Newborn Neurons

FXR2P-deficient (*Fxr2 KO*) mice have no apparent deficits in neuronal production either during development (Bontekoe et al., 2002) or as adults (Figure S1A–D), yet these mice exhibit significant learning and cognitive deficits (Bontekoe et al., 2002; Spencer et al., 2006). We found that *Fxr2 KO* mice were impaired in their performance of the delayed non-matching to place-radial arm task and trace conditioned learning task (Figure S1E–G) known to be dependent on postnatal neurogenesis (Guo et al., 2011a). To determine whether FXR2P deficiency affected maturation of new neurons, we stereotaxically injected retroviruses expressing GFP (CAG-GFP) into the dentate gyrus (DG), one of the neurogenic zones in the adult brain. The retrovirus targets only dividing cells therefore labels dividing neural progenitors in the DG and their subsequent progenies (Figure 1A)(Smrt et al., 2010). At 2 and 4 weeks post-injection (wpi), the dendritic arborization of GFP^+ newborn neurons was examined and quantified in 3D using confocal microscopy coupled to Neurolucida™ software. Newborn neurons in the adult DG of *Fxr2* KO mice had shorter dendrites at both 2 wpi (Figure 1B,C) and 4 wpi (Figure 1E,F) and are less complex at both 2 wpi (Figure 1D) and 4 wpi (Figure 1G) compared with WT mice. To confirm these defects were specific to FXR2P deficiency in adult-born neurons, we acutely knocked down FXR2P in the adult neural progenitors using a retrovirus expressing short hairpin RNA against FXR2P (*shFxr2*, Figure 1A and Figure S1H–O) (Guo et al., 2011b). Acute knockdown of FXR2P also resulted in shortened dendrites (Figure 1H, J) and reduced complexity (Figure 1I, K) in new neurons at both 2 wpi and 4 wpi. The density of dendritic spines of GFP+ new DG neurons at 4 wpi was significantly higher in FXR2P-deficient new neurons (Figure S1P–R), similar to what we had found in FMRP-deficient new adult neurons (Guo et al., 2011a; Guo et al., 2012). Furthermore, acute knockdown of FXR2P during embryonic development also led to similar dendritic maturation deficits in cortical neurons (Figure S2), suggesting that FXR2P likely has similar functions in neuronal maturation both during development and in adults For subsequent in vivo neuronal developmental studies, we used adult DG neurogenesis as the model because retrovirus-based single-cell genetics allows us to track the developmental process of single DG neurons.

Adult new neurons integrate into the hippocampal circuitry (Song et al., 2012). We reasoned that the impaired dendritic maturation of newborn neurons in *Fxr2* KO mice would lead to altered neural circuitry integration. We used a pseudo-typed rabies virus-based monosynaptic retrograde tracing method (Vivar et al., 2012; Wickersham et al., 2007) to map presynaptic partners of new DG neurons (Figure 2A, B). Newborn neurons were labeled by stereotaxic injection of a retrovirus (RV-Syn-GTRgp) expressing nuclear GFP (G), chicken virus receptor (TVA, or T), and rabies glycoprotein (Rgp) under the control of a synapsin (Syn) promoter.(Vivar et al., 2012; Wickersham et al., 2007) At 30 days post-retroviral injection, when new neurons started network integration, we gave mice one injection of chicken viral glycoprotein (EnvA)-pseudo-typed rabies virus (EnvA-ΔG-mCh), in which Rgp was replaced with mCherry (mCh). (Vivar et al., 2012; Wickersham et al., 2007). EnvA-ΔG-mCh selectively infects new neurons expressing TVA, complements with Rgp, crosses synapses, and labels the presynaptic neurons with mCh. Due to the absence of Rgp in the presynaptic neurons, this virus cannot spread further. Retrograde tracings were analyzed at 7 days after the rabies virus injection. We first validated this system using a control retrovirus missing Rgp (RV-Syn-GT) and found that this virus did not spread (data not shown), consistent with literature (Vivar et al., 2012). As expected, GFP^+ (green, new neurons without rabies virus infection) and GFP^+mCh^+ (yellow, rabies virus-infected new neurons “Starter Cells”) neurons were found in the DG, but mCh+ only (red “Traced Cells”) neurons were found in several other brain regions (Figure 2C,D). The ratio of Traced/Starter cells indicates the connectivity of retroviral-labeled adult-born new neurons. FXR2P deficiency led to a decreased connectivity overall (Figure 2E), as well as in specific regions (Figure 2F). Therefore, FXR2P-deficient new neurons with shorter dendrites connect to fewer presynaptic neurons.

FXR2P Enhances GluA1 Expression by Stabilizing Its mRNA

We next investigated the molecular mechanism underlying FXR2P regulation of neuronal maturation. We decided to focus on glutamate and GABA neural transmitter systems because they are known to regulate neuronal maturation during development (Smrt and Zhao, 2010; Song et al., 2012), and FXR2P deficiency affects the expression of these genes (Cavallaro et al., 2008). Using pathway arrays we found only a small number of genes exhibited more than 2-fold changes in *Fxr2* KO mice (Figure S3A). Arginine vasopressin (*Avp*) and metabotropic glutamate receptor 6 (*Grm6*) exhibited >2-fold higher levels, and ionotropic glutamate receptor AMPA1 (*GluA1* or *Gria1*) displayed >2-fold reduced levels in the DG of *Fxr2* KO mice (Figure S3B).

FXR2P is known to regulate gene expression by binding to its targeted mRNAs (Darnell et al., 2009; Guo et al., 2011b). Using FXR2P RNA immunoprecipitation (RNA-IP) followed by PCR, we found that FXR2P bound to *GluA1* mRNA and, as expected, *Noggin* mRNA (Guo et al., 2011b) (Figure 3A,B, Figure S3C), but not *Grm6* or *Avp* mRNAs (Figure S3C). We then confirmed that both *GluA1* mRNA levels (Figure 3C) and GluA1 protein levels (Figure 3D) were decreased in the *Fxr2* KO tissue compared to WT DG tissue. In contrast, GluA2, GABRG2, and GABBR1 protein levels exhibited no change in *Fxr2* KO mice (Figure S3D–F). Next, we treated FXR2P-deficient (*shFxr2* or *Fxr2* KO) neurons with actinomycin D to inhibit gene transcription and determined the stability of *GluA1* mRNA

over a 6-hour period using qPCR. We found that *GluA1* mRNA had a significantly reduced half-life in FXR2P-deficient neurons (Figure 3E, *shFxr2*, $T_{1/2}$ = 2.9 hours; Figure S4A, *Fxr2* KO, $T_{1/2}$ = 3.4 hours) compared to controls (Figure 3E, *shNC*, $T_{1/2}$ = 4.5 hours; Figure S4A *WT*, $T_{1/2}$ = 4.6 hours). The decay kinetics of control *Gapdh* mRNA was not significantly different between WT and KO (Figure S4B), suggesting that FXR2P regulates GluA1 expression by stabilizing its mRNA.

FXS proteins may bind both protein-coding sequences (CDS) and untranslated regions (UTRs) of mRNAs (Ascano et al., 2012; Darnell et al., 2011). To identify the regions of *GluA1* mRNA that might interact with FXR2P, we cloned 3 fragments ($CDS_{1\text{-}900}$, $CDS_{900\text{-}1800}$, and $CDS_{1800\text{-}2720}$) that together encompass the entire CDS and the 3′UTR of *GluA1* (Figure 3F) into luciferase reporter plasmids so that Renilla luciferase (R-luc) expression was regulated through the GluA1 fragments. We found the $CDS_{1\text{-}900}$ and $CDS_{900\text{-}1800}$ responded to the overexpression of FXR2P (Figure 3G), which was abolished by FXR2P acute knockdown (Figure 3H, I). We then confirmed the above results using a direct mRNA pull-down assay. We found that the in vitro-transcribed mRNA fragments containing the CDS of *GluA1* were bound by FXR2P in brain lysate, whereas the RNA fragment containing the *GluA1* 3′UTR was not (Figure 3J). In contrast, the *GluA1* mRNA was not bound by FMRP (Figure 3J), which is consistent with published literature (Darnell et al., 2011; Nakamoto et al., 2007; Zalfa et al., 2007). These data suggest that FXR2P may regulate *GluA1* mRNA stability by interacting with 1–1800 nucleotides of the CDS within *GluA1* mRNA.

The reduced GluA1 protein expression in *Fxr2* KO neurons could also result from either reduced protein translation or increased protein degradation. We treated *Fxr2* KO and WT neurons with the protein synthesis inhibitor cycloheximide for an 8-hour period and found no significant difference in the rate of GluA1 protein degradation between WT and KO neurons (Figure S4C–E). We then used a photo-convertible protein, Dendra II, to assess GluA1 protein synthesis and degradation (Figure 3K,L, Figure S4F). Dendra II changes from a 488-nm excitation fluorescence (green) to a 568-nm excitation fluorescence (red) upon UV conversion. Therefore, green fluorescence can be used to monitor newly synthesized protein, and red fluorescence can be used to show the degradation of existing protein. We transfected plasmids expressing DendraII-GluA1 fusion proteins into *Fxr2* KO or WT hippocampal neurons. After UV conversion, we monitored the fluorescence intensities over a 60-min period and found that neither the recovering rate of green fluorescence nor the decreasing rate of red fluorescence was significantly different between *Fxr2* KO and WT hippocampal neurons in either cell bodies (Figure 3L–N, Figure S4F, G) or dendrites (Figure S4H–J). Therefore FXR2P deficiency may not affect GluA1 protein synthesis and degradation. In addition, in FXR2P-deficient cells, there was a marginal reduction in the stability of *DendraII-GluA1* fusion mRNA ($p = 0.054$) but not *DendraII* mRNA ($p = 0.94$) compared to those in WT cells (Figure S4K,L). Taken together, our results suggest FXR2P regulates GluA1 expression mainly by binding to the CDS of *GluA1* mRNA and enhancing mRNA stability.

Restoration of GluA1 Expression Rescues the Dendritic Morphology Deficits of FXR2P-Deficient Neurons

The function of GluA1 in neuronal dendrite development during postnatal neurodevelopment is unknown. We first characterized GluA1 expression in the adult DG (Figure S5A). We found that GluA1 was absent in Ki67+ dividing cells, but present in a subset of DCX+ immature neurons and nearly all NeuN+ mature neurons (Figure S5B–D). To further characterize the timing of GluA1 expression, we stereotaxically injected retroviruses expressing GFP into the DG of adult mice to date the birth of the newborn neurons (Figure S5A). We found that GluA1 was not expressed in GFP+ cells at 1 wpi, when the majority of retrovirus-infected cells were either progenitors or at the initial neuronal differentiation stage. We detected GluA1 expression in GFP+ cells at 2 wpi (Figure S5E, F), when most infected cells had differentiated into neurons and were undergoing maturation.

We reasoned that GluA1 expression during this stage might have a significant role in maturation of new neurons. We injected retrovirus expressing GluA1 shRNA (*shGluA1*) into the adult DG to knock down GluA1 expression in new neurons (Figure 4A and Figure S5G–M). Knockdown of GluA1 in newborn neurons led to shorter dendrites and reduced dendritic complexity at both 2 wpi (Figure 4B, C) and 4 wpi (Figure 4D, E) compared with *shNC* controls. These data suggest GluA1 plays an important role in dendritic development during adult hippocampal neurogenesis.

Based on our data, we hypothesized that reduced dendritic complexity in FXR2P-deficient mice may be due to reduced GluA1 expression. If so, exogenous GluA1 should rescue the dendrite development of newborn neurons in *Fxr2* KO mice. We stereotaxically injected retroviruses expressing GluA1 as well as GFP (Figure 4F) into the DG of adult mice and analyzed at 2 and 4 wpi. We found that exogenous GluA1 enhanced dendritic length and complexity at both 2 wpi (Figure 4G–I) and 4 wpi (Figure 4J–L) in WT mice. More importantly, exogenous GluA1 indeed rescued the dendritic length (Figure 4H,K) and dendritic complexity (Figure 4I,L) of FXR2P-deficient newborn neurons in adult DG. Thus, restoration of GluA1 expression in newborn neurons of the adult DG could rescue the deficits in dendritic development due to a loss of FXR2P. Furthermore, double deletion of both FXR2P and GluA1 led to similar dendritic morphological defects as knocking down either FXR2P or GluA1 (Figure S5N, O). These data therefore support our hypothesis that FXR2P regulates neuronal maturation through GluA1.

Reduced Synaptic GluA1-Mediated AMPA Current in FXR2P-Deficient Neurons

We next wanted to investigate whether FXR2P-regulated GluA1 expression had an impact on synaptic transmission in new neurons, so we first assessed whether FXR2P deficiency affects the membrane surface expression of GluA1. *Fxr2* KO mice had a significant reduction in both total and membrane GluA1 (surface GluA1 or sGluA1) levels compared to WT mice (Figure 5A,B). However, the ratio of membrane versus total GluA1 did not differ significantly between WT and *Fxr2* KO mice (Figure 5C). These results suggest that FXR2P regulates the expression rather than membrane trafficking of GluA1 proteins. Since FXR2P deficiency only affects GluA1 but not GluA2 (Figure S3) levels, we next investigated

whether *Fxr2* KO neurons had reduced GluA1-mediated AMPA current. To distinguish GluA1-mediated AMPA receptor current from those mediated by other AMPA receptors, particularly GluA2/3 AMPA receptors, we employed a method to specifically determine the contribution of GluA1-containing AMPA receptors among total synaptic AMPA receptors (Kielland et al., 2009; McCormack et al., 2006). We used recombinant Sindbis virus to express a GFP-tagged cytoplasmic terminus of GluA1 (GluA1ct-GFP), a dominant-negative construct that selectively blocks synaptic trafficking of endogenous GluA1 in DG neurons and analyzed at ~16 h after viral delivery. We stimulated the afferent perforant path fibers in the DG and recorded the evoked excitatory postsynaptic currents (EPSCs) in DG neurons. If GluA1 contributes significantly to synaptic AMPA current, we should see a reduction of AMPA current by GluA1ct-GFP expression. Indeed, WT DG neurons infected with GluA1ct-GFP virus exhibited ~25% reduced AMPA responses compared to nearby uninfected neurons (Figure 5E–G), pointing to a significant contribution of GluA1-containing AMPA receptors to synaptic transmission in WT DG neurons. In contrast, *Fxr2* KO DG cells expressing GluA1ct-GFP did not exhibit significantly reduced AMPA current compared to nearby uninfected neurons, suggesting that *Fxr2* KO neurons had reduced involvement from GluA1-containing AMPA receptors in synaptic transmission. As expected, GluA1ct-GFP had no effect on NMDA current in either WT or KO DG neurons (Figure 5G,H). Together, these results indicate that FXR2P deficiency leads to reduced stability of *GluA1* mRNA leading to reduced cell surface levels of GluA1 proteins and reduced GluA1-mediated synaptic transmission.

FXR2P and FMRP Additively Regulate Membrane GluA1 Levels

Although FMRP does not regulate GluA1 expression levels, FMRP deficiency leads to reduced membrane and synaptic delivery of GluA1 and hence reduced GluA1-mediated AMPA current (Hu et al., 2008; Lim et al., 2014; Nakamoto et al., 2007). Indeed, we found that *Fmr1* KO mice had comparable total GluA1 expression levels, but greatly reduced membrane GluA1 levels compared with WT mice. Therefore, the ratio of membrane versus total GluA1 was decreased in *Fmr1* KO neurons compared to WT (Figure S6), consistent with previous findings (Hu et al., 2008; Nakamoto et al., 2007). These results suggest that FMRP and FXR2P regulate GluA1 via distinct mechanisms. (Spencer et al., 2006; Zhang et al., 2009)

We next investigated whether both FMRP and FXR2P regulate the membrane availability of GluA1 in neurons lacking FXR2P, FMRP, or both. We labeled the cell surface proteins with biotin and the amount of cell surface GluA1 in biotin-labeled fractions was assessed using Western blot. Consistent with the above results, we found *Fmr1* KO neurons had significantly reduced surface GluA1, but not total GluA1, compared with WT neurons (Figure 6A–C). On the other hand, the FXR2P-deficient neurons (*shFxr2*) had a significant reduction in both surface and total GluA1 levels compared with WT neurons (Figure 6A–C). The ratio of surface versus total GluA1 was reduced in *Fmr1* KO neurons, but not *Fxr2* KO neurons (Figure 6C). Therefore, deficiency in either FXR2P or FMRP leads to reduced surface GluA1 levels in primary neurons, similar to levels in mouse brains (Figure 5A–C and Figure S6). Next we investigated the synergistic effect of FXR2P and FMRP by acutely knocking down FXR2P in *Fmr1* KO neurons. We found that membrane GluA1 levels were

significantly reduced in FMRP and FXR2P double-mutant neurons compared with FXR2P and FMRP single-mutant neurons (Figure 6A–C). Thus, both FMRP and FXR2P regulate the surface GluA1 levels in neurons but via distinct mechanisms.

To confirm the additive effect of FXR2P and FMRP in regulating the cell surface levels of GluA1 in new neurons in vivo, we stereotaxically injected a retrovirus expressing a pH-sensitive GFP-GluA1 fusion protein (pHlourin-GluA1) (Makino and Malinow, 2009) together with a retrovirus expressing either *shFmr1* or *shNC* (and RFP) into the DG of WT and *Fxr2* KO adult mice (Figure 6D). At 4 wpi, we analyzed cell surface GluA1 expression in RFP+ new neurons by staining brain sections with an anti-GFP antibody that could recognize pHlourin under cell impermeable conditions (Figure 6E,F). As expected, the surface GluA1 levels in FXR2P or FMRP single-deficient neurons showed a significant reduction compared with WT neurons (Figure 6G). More importantly, the surface GluA1 levels in the double-deficient newborn neurons were significantly reduced compared with single-deficient newborn neurons (Figure 6K). Therefore, FXR2P and FMRP have an additive effect on GluA1 surface levels in adult-born neurons in the DG.

FXR2P and FMRP Exhibit an Additive Effect on the Dendritic Development of New Neurons

Since FXR2P and FMRP had an additive effect on membrane GluA1 expression, we hypothesized that FXR2P and FMRP would have an additive effect on the dendritic arborization of adult DG newborn neurons. We therefore injected retroviruses expressing *shFmr1* into the DG of *Fxr2* KO mice and analyzed new neurons at 4 wpi (Figure 7A, Figure S7). Consistent with our previous findings (Guo et al., 2011a), knocking down FMRP in adult newborn DG neurons led to shorter dendrites (Figure 7B) and reduced dendritic complexity (Figure 7C) compared with WT mice. More importantly, FMRP and FXR2P double-deficient neurons had significantly shorter dendrites (Figure 7B) and reduced dendritic complexity (Figure 7C) compared to single-mutant mice. Therefore, FMRP and FXR2P exhibit an additive effect on neuronal dendritic maturation.

We hypothesized that a reduction of GluA1 levels in FMRP-deficient neurons should mimic FMRP and FXR2P double knockout. Thus, we injected retroviruses expressing *shGluA1* into the DG of adult *Fmr1* KO mice and analyzed them at 4 wpi (Figure 7D, Figure S7). We found that knockdown of GluA1 in newborn neurons of *Fmr1* KO mice led to further reductions in dendritic length (Figure 7E) and dendritic complexity (Figure 7F) compared with either *Fmr1* KO neurons or *shGluA1*-infected WT neurons. Thus, the additive effect of FMRP and FXR2P on the dendritic maturation of newborn neurons occurs via distinct regulatory mechanisms converging on GluA1 (Figure 7G).

DISCUSSION

Although altered neuronal and synaptic patterning has been associated with many neurological and psychiatric illnesses, the underlying molecular mechanism is far from clear. Our study therefore provides fresh insight into regulatory mechanisms governing neurogenesis and sheds light on how critical neurodevelopmental regulators may additively contribute to the pathogenesis of human diseases.

First, our studies unveil distinct functions and a functional convergence of FXR proteins

Although FMRP is unique in its ability to recognize G-quadruplexes, all three FXR proteins can bind kissing complex RNAs through their conserved KH2 domain (Darnell et al., 2009). However, the two exons present in the KH2 domain of FMRP are absent in FXR1P and FXR2P. Further, FXR1P and FXR2P have nucleolar localization signals that are lacking in FMRP. The functional specificity and redundancy of FXRs are largely unknown. *Drosophila melanogaster* has one *dFMR1* gene, whereas mammals have three paralogs. The contributions of FXR1P and FXR2P make to FXS are unclear. FXR1P mutation is perinatal lethal, whereas FXR2P mutation yields behavioral phenotypes similar to *Fmr1* KO mice (Bontekoe et al., 2002; Mientjes et al., 2004). The relatively mild phenotypes seen in *Fmr1* KO mice compared to *dFmr1* mutant *Drosophila* and human FXS patients suggest the potential contribution of other FXRs to FXS. In either FMRP or FXR2P knockout brain tissues or cells, there is no compensatory increase of the other FXR (Guo et al., 2011b; Luo et al., 2010), suggesting they may function differently. Loss of FMRP expression enhances mGluR-dependent long-term depression (LTD) that is independent of protein synthesis. Whereas, *Fxr2* KO mice have decreased mGluR-LTD that remains protein synthesis-dependent (Zhang et al., 2009). We found that FMRP deficiency leads to decreased neuronal differentiation (Guo et al., 2011a; Guo et al., 2012; Luo et al., 2010), whereas FXR2P mutation leads to increased neuronal differentiation (Guo et al., 2011b) of adult neural stem cells. Here we show that FXR2P binds to *GluA1* mRNA, whereas FMRP does not (Darnell and Klann, 2013; Darnell et al., 2011). On the other hand, GluA1 membrane delivery is regulated by FMRP (Hu et al., 2008; Nakamoto et al., 2007), but not FXR2P. Therefore, the two FXRs regulate GluA1 through distinct mechanisms. Reduced GluA1 membrane expression could result in the exaggerated LTD seen in double-mutant mice (Zhang et al., 2008; Zhang et al., 2009).

The dynamic regulation of AMPAR trafficking to the plasma membrane at glutamatergic synapses plays critical roles in the long-term synaptic plasticity underlying learning and memory. We know that FMRP has significant roles in regulating the synaptic delivery of GluA1 (Hu et al., 2008; Nakamoto et al., 2007). Although FMRP does not directly bind *GluA1* mRNA, it regulates many synaptic proteins in the NMDA-R—Ras—PI3K/PKB signaling interactome (Ascano et al., 2012; Darnell and Klann, 2013; Kielland et al., 2009), which modulate synaptic trafficking of GluA1 (Lim et al., 2014; Soden and Chen, 2010). FMRP is also known to repress the synthesis proteins involved in LTD, such as activity-regulated cytoskeleton-associated protein (Arc), striatal-enriched protein tyrosine phosphatase (STEP), microtubule-associated protein 1B (MAP1B) and upregulation of these “LTD proteins” likely play roles in AMPA receptor trafficking (Darnell et al., 2011; Waung and Huber, 2009). However, the role of other FXRs in this process has yet to be explored. It is interesting that we discovered another FXR protein that also regulates GluA1. The fact that the two FXR proteins regulate the same GluA1 via distinct mechanisms makes it possible for potential functional cooperation. Such additive actions of the two FXR proteins may take on a different flavor in other cell types or physiological processes.

Second, our study unveils a role of AMPA receptor during neuronal development

AMPA-type glutamate receptors are involved in fast excitatory transmission in the mammalian central nervous system, which is important for neuronal development and inter-neuronal connectivity (Hamad et al., 2011; Urbanska et al., 2008). Studies have revealed that loss of GluA1 in developing neurons reduces dendritic complexity, whereas overexpression of GluA1 increases it (Hamad et al., 2011; Srivastava et al., 2012). Although GluA1 is found in immature adult-born neurons (Hagihara et al., 2011), its function in adult neurogenesis was unexplored. (Hagihara et al., 2011). We found that GluA1 is also expressed in immature adult-born neurons and regulates neuronal maturation. Therefore, the function of GluA1 in promoting neuronal maturation is conserved from development to adulthood. Both GABA and NMDA receptors are known to play intrinsic roles in the development of adult new neurons (Ge et al., 2006; Kheirbek et al., 2012; Platel et al., 2008; Platel et al., 2010; Tozuka et al., 2005). Adult new neurons develop within the niche formed by many mature neurons therefore the precisely controlled expression of neurotransmitter receptors may shape the maturation of young neurons by allowing these new neurons to receive signals from their niche. Since the development and integration of DG new neurons are regulated by neuronal activities(Ming and Song, 2011), it is not surprising that inhibition of GluA1 synaptic integration affects basal synaptic transmission in developing DG neurons (Figure 5). These results are consistent with the activity dependence of GluA1 synaptic integration (Kopec et al., 2007; Stornetta and Zhu, 2011). Future development in this research area will help us come to a more complete understanding of this regulatory mechanism. Notably, the effect of GluA1 on dendritic development may not be solely via its synaptic function. It is possible that non-synaptic GluA1 may also play important roles in dendritic maturation, which may explain why dominant GluA1ct-GFP did not suppress the remaining GluA1 current in FXR2P mutant neurons (Figure 5).

Third, our study has uncovered a regulatory mechanism that controls GluA1 expression

GluA1 is regulated at multiple levels, including transcription, splicing, translation, and membrane trafficking (Kessels and Malinow, 2009). In this study, we discovered a new regulatory mechanism of GluA1, which is through mRNA stability. FXR proteins are known to act mainly as translational repressors for protein synthesis (Darnell et al., 2009; Darnell et al., 2011; Guo et al., 2011b). However, several recent studies suggest that FXR can also regulate the stability of the mRNAs, leading to a subsequent increase or decrease in protein production. For example FMRP has been shown to increase the stability of PSD95 mRNA (Zalfa et al., 2007). We have shown that FXR2P reduces Noggin mRNA stability in adult neural stem cells (Guo et al., 2011b). Here we show that the same FXR2P protein binds to GluA1 mRNA and enhances its stability and protein production. How FXRs select their mRNA targets is largely unclear, but why FXRs can stabilize certain mRNAs yet destabilize other mRNAs is even less well understood. The fact that FXRs can bind the entire coding sequence (Ascano et al., 2012; Darnell et al., 2011) suggests other co-factors may be needed for their specificity and mechanisms of action. Future studies of co-factors help FXRs to select the mode of action should be a fruitful area of research.

Fourth, our data emphasize the importance of dendritic maturation in neural network integration

The impact of altered dendritic arborization on neural network integration is largely unknown. For example, in the context of adult neurogenesis, the number of new neurons seems to be the critical regulatory point in both health and disease (Ge et al., 2008; Zhao et al., 2008). Although a number of studies have shown altered dendritic morphogenesis of adult-born new neurons in disease models, only limited studies (Duan et al., 2007)demonstrate that new neurons with impaired dendritic development leads to impaired excitability and functional synapse formation (Duan et al., 2007). The recently developed rabies virus-mediated retrograde synaptic tracing method (Vivar et al., 2012; Wickersham et al., 2007) allowed us to assess the presynaptic connection onto new neurons that lack FXR2P. Several variations of this rabies virus retrograde tracing system have been applied to map presynaptic connections onto adult-born new neurons (Deshpande et al., 2013; Li et al., 2013; Vivar et al., 2012). To our surprise, with a seemingly mild reduction in dendritic length and complexity, these FXR2P-deficient new neurons exhibited 70% reduced connectivity compared to WT neurons (Figure 2). Therefore, even mildly reduced neuronal maturation may have a serious impact on network integration. The acute knockdown of FXR2P in developing neurons also led to profound dendritic arborization deficiency (Figure S2), suggesting that, although FXR2P mice exhibit no significant changes in brain structure, their neuronal network integration might be defective. As the next step, it will be interesting to explore which specific presynaptic inputs are affected in FXR2P-deficient mice. The cell types and numbers of presynaptic neurons connected to adult-born new neurons change during neuronal maturation (Vivar et al., 2012),. It will be important to evaluate these dynamic changes in genetic disease models, as well as to evaluate how much the impaired dendritic spine maturation we saw contributes to the reduced network integration of FXR2P mutant neurons. Our data establish an important role for dendritic maturation in the network integration of new neurons during adult neurogenesis.

METHODS

(See Supplemental Methods for details)

Mice

All animal procedures were approved by University of Wisconsin-Madison Care and Use Committee. The *Fxr2 KO* mice (C57B/L6 strain) were described previously (Bontekoe et al., 2002). The Fmr1 KO mice (C57B/L6 strain) were described previously (1994; Luo et al., 2010).

DNA Plasmids

GluA1 fragments were amplified by PCR and cloned into a pSicheck2 dual luciferase vector (Invitrogen) or a Dendra-2 C1 vector (Evogen). Retroviral vector expressing pHlourin-GluA1 was cloned from pRK5.pHluorin-GluA1 plasmid (Makino and Malinow, 2009) (a gift from Dr. RL Huganir, Johns Hopkins University) into CAG-GFP retroviral vector (Smrt et al., 2010). Retroviral vector expressing GluA1, (Smrt et al., 2010), shRNA-insensitive GluA1 (mtGluA1) and shRNA-insensitive FXR2 (mtFXR2) were created by PCR and

cloned into CAG-GFP retroviral vector. RV-Syn-GTRgp retroviral vector was a general gift from Drs van Praag (NIH), Suh (Cleveland Clinic) and Gage (Salk Institute) (Vivar et al., 2012).

RNA Immunoprecipitation

RNA-IP was performed as described(Guo et al., 2011b)

mRNA Stability Assay

Culture hippocampus neurons were treated with 10 mg/ml of actinomycin D (Sigma-Aldrich) to inhibit gene transcription as described(Guo et al., 2011b) and neurons were collected at various time intervals for RNA isolation and real time PCR analysis. *GluA1* mRNA levels were normalized to *Gapdh*. RNA decay kinetics and half-life were analyzed using published method(Beckel-Mitchener et al., 2002)

Biotin- mRNA Pull-Down Assay

In vitro transcription of biotin-labeled GluA1 RNA and pull down were carried as previously published (Guo et al., 2011b). The proteins in the pull-down material were separated by 4–20% SDS-PAGE gel, transferred to nitrocellulose membrane for Western blot analysis using an anti-FXR2 antibody or anti-FMRP antibody.

Viral Production and in vivo Grafting

Production of Lentivirus and retrovirus and in vivo grafting were performed as described (Smrt et al., 2010). The glycoprotein–gene-deleted rabies virus stock (Δgp-mCh) was a general gift from Dr. Gallaway (Salk Institute). The production of pseudotyped rabies virus was carried out as described previously (Vivar et al., 2012; Wickersham et al., 2007). Mice were injected with rabies virus at 30 days after retroviral injections.

3D dendritic morphological analysis of new neurons

3D analyses of neuronal dendrites were performed as described (Smrt et al., 2010). 300-μm-thick floating brain sections were imaged on a Nikon A1 confocal or a Zeiss Aptome microscope with a 20 X objective. Z-stacks of eGFP+ or RFP+ dendrites were captured and the dendrites and analyzed by Neurolucida software (MicroBrightField, Inc. Williston, VI). Roughly 20–30 neurons per DG were traced.

Rabies virus-based retrograde tracing

The numbers of GFP^+mCh^+ and mCh^+ cells were quantified in 1:6 series of coronal sections (40 μm) through the dorsal–ventral extent of the brain. The ratio of mCh^+ over GFP^+mCh^+ was used to determine the connectivity of newborn neurons in the DG.

Cell Surface GluA1 Analysis

Isolation of cell surface protein and western blot analysis of biotinylated surface GluA1 were performed as described (Soden and Chen, 2010). For histological assessment of retro-pHlorinGFP-GluA1 labeled new neurons, brain sections were stained with a chicken monoclonal anti-GFP antibody (Invitrogen, 1:1000) followed by incubation with an anti-

mouse Alexa 647-conjugated secondary antibody (Invitrogen) in cell impermeable (detergent-free) condition. The mean red (RFP) and far-red fluorescence intensity (surface GluA1) was obtained using NIS-Elements C software. The surface GluA1 expression was determined by mean far-red fluorescence over red fluorescence.

GluA1 Synaptic Current Analysis

GluA1ct-GFP (Hu et al., 2008; Kielland et al., 2009; Qin et al., 2005)was expressed in hippocampal DG neurons of postnatal 17–21 days old mice using Sindbis virus as described (Hu et al., 2008).. About 16 h after viral injections, acute hippocampal slices were prepared from these animals for *in vitro* electrophysiology experiments. Simultaneous whole-cell recordings were obtained from nearby infected and control non-infected hippocampal DG neuron pairs

Statistical Analysis

Statistical analysis was performed using ANOVA and Student's t test, unless specified, with the aid of SPSS version 22 and Graphpad software. Two tailed and unpaired t-test was used to compare two conditions. One-Way ANOVA was used for comparison among multiple experimental conditions. Bonderroni post hoc test was used when compare among each condition. Whereas Dunnett post hoc test was used when compare multiple conditions to the same control. Scholl analysis was carried out using a multivariate analysis of variance (MANOVA) using SPSS statistical software. All data were shown as mean with standard error of mean (mean ± SEM). Probabilities of $p < 0.05$ were considered as significant.

Supplementary Material

Refer to Web version on PubMed Central for supplementary material.

Acknowledgments

We thank C.T. Strauss for editing, Y. Xing for technical assistance, and the Zhao lab members for discussion. We thank Dr. J. Zhu for use of lab resources and consultation. This work was supported by grants from the NIH (R01MH080434 and R01MH078972 to X.Z.), the International Rett Syndrome Foundation (IRSF, 2755 to X.Z.), FRAXA (to X.Z.), and a Center grant from the NIH to the Waisman Center (P30HD03352). W.G. was funded by a postdoctoral fellowship from the UW Center for Stem Cells and Regenerative Medicine. E.D.P. was funded by a UW Hilldale fellowship for undergraduate research. G.W. was supported in part by a grant from the Epilepsy Foundation (No. 310443).

References

1. The Dutch-Belgian Fragile X Consortium. Fmr1 knockout mice: a model to study fragile X mental retardation. Cell. 78:23–33.
2. Akins MR, Leblanc HF, Stackpole EE, Chyung E, Fallon JR. Systematic mapping of fragile X granules in the mouse brain reveals a potential role for presynaptic FMRP in sensorimotor functions. J Comp Neurol. 2012; 520:3687–3706. [PubMed: 22522693]
3. Ascano M Jr, Mukherjee N, Bandaru P, Miller JB, Nusbaum JD, Corcoran DL, Langlois C, Munschauer M, Dewell S, Hafner M, et al. FMRP targets distinct mRNA sequence elements to regulate protein expression. Nature. 2012; 492:382–386. [PubMed: 23235829]
4. Beckel-Mitchener AC, Miera A, Keller R, Perrone-Bizzozero NI. Poly(A) tail length-dependent stabilization of GAP-43 mRNA by the RNA-binding protein HuD. J Biol Chem. 2002; 277:27996–28002. [PubMed: 12034726]

5. Bontekoe CJ, McIlwain KL, Nieuwenhuizen IM, Yuva-Paylor LA, Nellis A, Willemsen R, Fang Z, Kirkpatrick L, Bakker CE, McAninch R, et al. Knockout mouse model for Fxr2: a model for mental retardation. Human molecular genetics. 2002; 11:487–498. [PubMed: 11875043]
6. Cavallaro S, Paratore S, Fradale F, de Vrij FM, Willemsen R, Oostra BA. Genes and pathways differentially expressed in the brains of Fxr2 knockout mice. Neurobiology of disease. 2008; 32:510–520. [PubMed: 18930145]
7. Darnell JC, Fraser CE, Mostovetsky O, Darnell RB. Discrimination of common and unique RNA-binding activities among Fragile X mental retardation protein paralogs. Human molecular genetics. 2009; 18:3164–3177. [PubMed: 19487368]
8. Darnell JC, Klann E. The translation of translational control by FMRP: therapeutic targets for FXS. Nat Neurosci. 2013; 16:1530–1536. [PubMed: 23584741]
9. Darnell JC, Van Driesche SJ, Zhang C, Hung KY, Mele A, Fraser CE, Stone EF, Chen C, Fak JJ, Chi SW, et al. FMRP stalls ribosomal translocation on mRNAs linked to synaptic function and autism. Cell. 2011; 146:247–261. [PubMed: 21784246]
10. Deshpande A, Bergami M, Ghanem A, Conzelmann KK, Lepier A, Gotz M, Berninger B. Retrograde monosynaptic tracing reveals the temporal evolution of inputs onto new neurons in the adult dentate gyrus and olfactory bulb. Proceedings of the National Academy of Sciences of the United States of America. 2013; 110:E1152–1161. [PubMed: 23487772]
11. Duan X, Chang JH, Ge S, Faulkner RL, Kim JY, Kitabatake Y, Liu XB, Yang CH, Jordan JD, Ma DK, et al. Disrupted-In-Schizophrenia 1 regulates integration of newly generated neurons in the adult brain. Cell. 2007; 130:1146–1158. [PubMed: 17825401]
12. Eisch AJ, Petrik D. Depression and hippocampal neurogenesis: a road to remission? Science. 2012; 338:72–75. [PubMed: 23042885]
13. Ge S, Goh EL, Sailor KA, Kitabatake Y, Ming GL, Song H. GABA regulates synaptic integration of newly generated neurons in the adult brain. Nature. 2006; 439:589–593. [PubMed: 16341203]
14. Ge S, Pradhan DA, Ming GL, Song H. GABA sets the tempo for activity-dependent adult neurogenesis. Trends Neurosci. 2007; 30:1–8. [PubMed: 17116335]
15. Ge S, Sailor KA, Ming GL, Song H. Synaptic integration and plasticity of new neurons in the adult hippocampus. J Physiol. 2008; 586:3759–3765. [PubMed: 18499723]
16. Guo W, Allan AM, Zong R, Zhang L, Johnson EB, Schaller EG, Murthy AC, Goggin SL, Eisch AJ, Oostra BA, et al. Ablation of Fmrp in adult neural stem cells disrupts hippocampus-dependent learning. Nature medicine. 2011a; 17:559–565.
17. Guo W, Murthy AC, Zhang L, Johnson EB, Schaller EG, Allan AM, Zhao X. Inhibition of GSK3beta improves hippocampus-dependent learning and rescues neurogenesis in a mouse model of fragile X syndrome. Human molecular genetics. 2012; 21:681–691. [PubMed: 22048960]
18. Guo W, Zhang L, Christopher DM, Teng ZQ, Fausett SR, Liu C, George OL, Klingensmith J, Jin P, Zhao X. RNA-binding protein FXR2 regulates adult hippocampal neurogenesis by reducing Noggin expression. Neuron. 2011b; 70:924–938. [PubMed: 21658585]
19. Hagerman RJ, Polussa J. Treatment of the psychiatric problems associated with fragile X syndrome. Curr Opin Psychiatry. 2015; 28:107–112. [PubMed: 25602250]
20. Hagihara H, Ohira K, Toyama K, Miyakawa T. Expression of the AMPA Receptor Subunits GluR1 and GluR2 is Associated with Granule Cell Maturation in the Dentate Gyrus. Frontiers in neuroscience. 2011; 5:100. [PubMed: 21927594]
21. Hamad MI, Ma-Hogemeier ZL, Riedel C, Conrads C, Veitinger T, Habijan T, Schulz JN, Krause M, Wirth MJ, Hollmann M, et al. Cell class-specific regulation of neocortical dendrite and spine growth by AMPA receptor splice and editing variants. Development. 2011; 138:4301–4313. [PubMed: 21865324]
22. Hu H, Qin Y, Bochorishvili G, Zhu Y, van Aelst L, Zhu JJ. Ras signaling mechanisms underlying impaired GluR1-dependent plasticity associated with fragile X syndrome. The Journal of neuroscience: the official journal of the Society for Neuroscience. 2008; 28:7847–7862. [PubMed: 18667617]
23. Kessels HW, Malinow R. Synaptic AMPA receptor plasticity and behavior. Neuron. 2009; 61:340–350. [PubMed: 19217372]

24. Kheirbek MA, Tannenholz L, Hen R. NR2B-dependent plasticity of adult-born granule cells is necessary for context discrimination. The Journal of neuroscience: the official journal of the Society for Neuroscience. 2012; 32:8696–8702. [PubMed: 22723709]
25. Kielland A, Bochorishvili G, Corson J, Zhang L, Rosin DL, Heggelund P, Zhu JJ. Activity patterns govern synapse-specific AMPA receptor trafficking between deliverable and synaptic pools. Neuron. 2009; 62:84–101. [PubMed: 19376069]
26. Kopec CD, Real E, Kessels HW, Malinow R. GluR1 links structural and functional plasticity at excitatory synapses. The Journal of neuroscience: the official journal of the Society for Neuroscience. 2007; 27:13706–13718. [PubMed: 18077682]
27. Li Y, Stam FJ, Aimone JB, Goulding M, Callaway EM, Gage FH. Molecular layer perforant path-associated cells contribute to feed-forward inhibition in the adult dentate gyrus. Proceedings of the National Academy of Sciences of the United States of America. 2013; 110:9106–9111. [PubMed: 23671081]
28. Li Y, Zhao X. Fragile X proteins in stem cell maintenance and differentiation. Stem Cells. 2014
29. Lim CS, Hoang ET, Viar KE, Stornetta RL, Scott MM, Zhu JJ. Pharmacological rescue of Ras signaling, GluA1-dependent synaptic plasticity, and learning deficits in a fragile X model. Genes Dev. 2014; 28:273–289. [PubMed: 24493647]
30. Luo Y, Shan G, Guo W, Smrt RD, Johnson EB, Li X, Pfeiffer RL, Szulwach KE, Duan R, Barkho BZ, et al. Fragile x mental retardation protein regulates proliferation and differentiation of adult neural stem/progenitor cells. PLoS genetics. 2010; 6:e1000898. [PubMed: 20386739]
31. Makino H, Malinow R. AMPA receptor incorporation into synapses during LTP: the role of lateral movement and exocytosis. Neuron. 2009; 64:381–390. [PubMed: 19914186]
32. McCormack SG, Stornetta RL, Zhu JJ. Synaptic AMPA receptor exchange maintains bidirectional plasticity. Neuron. 2006; 50:75–88. [PubMed: 16600857]
33. Mientjes EJ, Willemsen R, Kirkpatrick LL, Nieuwenhuizen IM, Hoogeveen-Westerveld M, Verweij M, Reis S, Bardoni B, Hoogeveen AT, Oostra BA, et al. Fxr1 knockout mice show a striated muscle phenotype: implications for Fxr1p function in vivo. Human molecular genetics. 2004; 13:1291–1302. [PubMed: 15128702]
34. Ming GL, Song H. Adult neurogenesis in the mammalian brain: significant answers and significant questions. Neuron. 2011; 70:687–702. [PubMed: 21609825]
35. Nakamoto M, Nalavadi V, Epstein MP, Narayanan U, Bassell GJ, Warren ST. Fragile X mental retardation protein deficiency leads to excessive mGluR5-dependent internalization of AMPA receptors. Proceedings of the National Academy of Sciences of the United States of America. 2007; 104:15537–15542. [PubMed: 17881561]
36. Platel JC, Dave KA, Bordey A. Control of neuroblast production and migration by converging GABA and glutamate signals in the postnatal forebrain. J Physiol. 2008; 586:3739–3743. [PubMed: 18467361]
37. Platel JC, Dave KA, Gordon V, Lacar B, Rubio ME, Bordey A. NMDA receptors activated by subventricular zone astrocytic glutamate are critical for neuroblast survival prior to entering a synaptic network. Neuron. 2010; 65:859–872. [PubMed: 20346761]
38. Qin Y, Zhu Y, Baumgart JP, Stornetta RL, Seidenman K, Mack V, van Aelst L, Zhu JJ. State-dependent Ras signaling and AMPA receptor trafficking. Genes Dev. 2005; 19:2000–2015. [PubMed: 16107614]
39. Sakai Y, Shaw CA, Dawson BC, Dugas DV, Al-Mohtaseb Z, Hill DE, Zoghbi HY. Protein interactome reveals converging molecular pathways among autism disorders. Sci Transl Med. 2011; 3:86ra49.
40. Smrt RD, Szulwach KE, Pfeiffer RL, Li X, Guo W, Pathania M, Teng ZQ, Luo Y, Peng J, Bordey A, et al. MicroRNA miR-137 regulates neuronal maturation by targeting ubiquitin ligase mind bomb-1. Stem Cells. 2010; 28:1060–1070. [PubMed: 20506192]
41. Smrt RD, Zhao X. Epigenetic regulation of neuronal dendrite and dendritic spine development. Front Biol. 2010; 5:304–323.
42. Soden ME, Chen L. Fragile X protein FMRP is required for homeostatic plasticity and regulation of synaptic strength by retinoic acid. The Journal of neuroscience: the official journal of the Society for Neuroscience. 2010; 30:16910–16921. [PubMed: 21159962]

43. Song J, Christian KM, Ming GL, Song H. Modification of hippocampal circuitry by adult neurogenesis. Developmental neurobiology. 2012; 72:1032–1043. [PubMed: 22354697]
44. Spencer CM, Serysheva E, Yuva-Paylor LA, Oostra BA, Nelson DL, Paylor R. Exaggerated behavioral phenotypes in Fmr1/Fxr2 double knockout mice reveal a functional genetic interaction between Fragile X-related proteins. Human molecular genetics. 2006; 15:1984–1994. [PubMed: 16675531]
45. Srivastava DP, Copits BA, Xie Z, Huda R, Jones KA, Mukherji S, Cahill ME, VanLeeuwen JE, Woolfrey KM, Rafalovich I, et al. Afadin is required for maintenance of dendritic structure and excitatory tone. J Biol Chem. 2012; 287:35964–35974. [PubMed: 22948147]
46. Stornetta RL, Zhu JJ. Ras and Rap signaling in synaptic plasticity and mental disorders. Neuroscientist. 2011; 17:54–78. [PubMed: 20431046]
47. Tozuka Y, Fukuda S, Namba T, Seki T, Hisatsune T. GABAergic excitation promotes neuronal differentiation in adult hippocampal progenitor cells. Neuron. 2005; 47:803–815. [PubMed: 16157276]
48. Urbanska M, Blazejczyk M, Jaworski J. Molecular basis of dendritic arborization. Acta neurobiologiae experimentalis. 2008; 68:264–288. [PubMed: 18511961]
49. Vivar C, Potter MC, Choi J, Lee JY, Stringer TP, Callaway EM, Gage FH, Suh H, van Praag H. Monosynaptic inputs to new neurons in the dentate gyrus. Nature communications. 2012; 3:1107.
50. Wang T, Bray SM, Warren ST. New perspectives on the biology of fragile X syndrome. Curr Opin Genet Dev. 2012; 22:256–263. [PubMed: 22382129]
51. Waung MW, Huber KM. Protein translation in synaptic plasticity: mGluR-LTD, Fragile X. Curr Opin Neurobiol. 2009; 19:319–326. [PubMed: 19411173]
52. Wickersham IR, Lyon DC, Barnard RJ, Mori T, Finke S, Conzelmann KK, Young JA, Callaway EM. Monosynaptic restriction of transsynaptic tracing from single, genetically targeted neurons. Neuron. 2007; 53:639–647. [PubMed: 17329205]
53. Zalfa F, Eleuteri B, Dickson KS, Mercaldo V, De Rubeis S, di Penta A, Tabolacci E, Chiurazzi P, Neri G, Grant SG, et al. A new function for the fragile X mental retardation protein in regulation of PSD-95 mRNA stability. Nat Neurosci. 2007; 10:578–587. [PubMed: 17417632]
54. Zhang J, Fang Z, Jud C, Vansteensel MJ, Kaasik K, Lee CC, Albrecht U, Tamanini F, Meijer JH, Oostra BA, et al. Fragile X-related proteins regulate mammalian circadian behavioral rhythms. Am J Hum Genet. 2008; 83:43–52. [PubMed: 18589395]
55. Zhang J, Hou L, Klann E, Nelson DL. Altered hippocampal synaptic plasticity in the FMR1 gene family knockout mouse models. Journal of neurophysiology. 2009; 101:2572–2580. [PubMed: 19244359]
56. Zhao C, Deng W, Gage FH. Mechanisms and functional implications of adult neurogenesis. Cell. 2008; 132:645–660. [PubMed: 18295581]

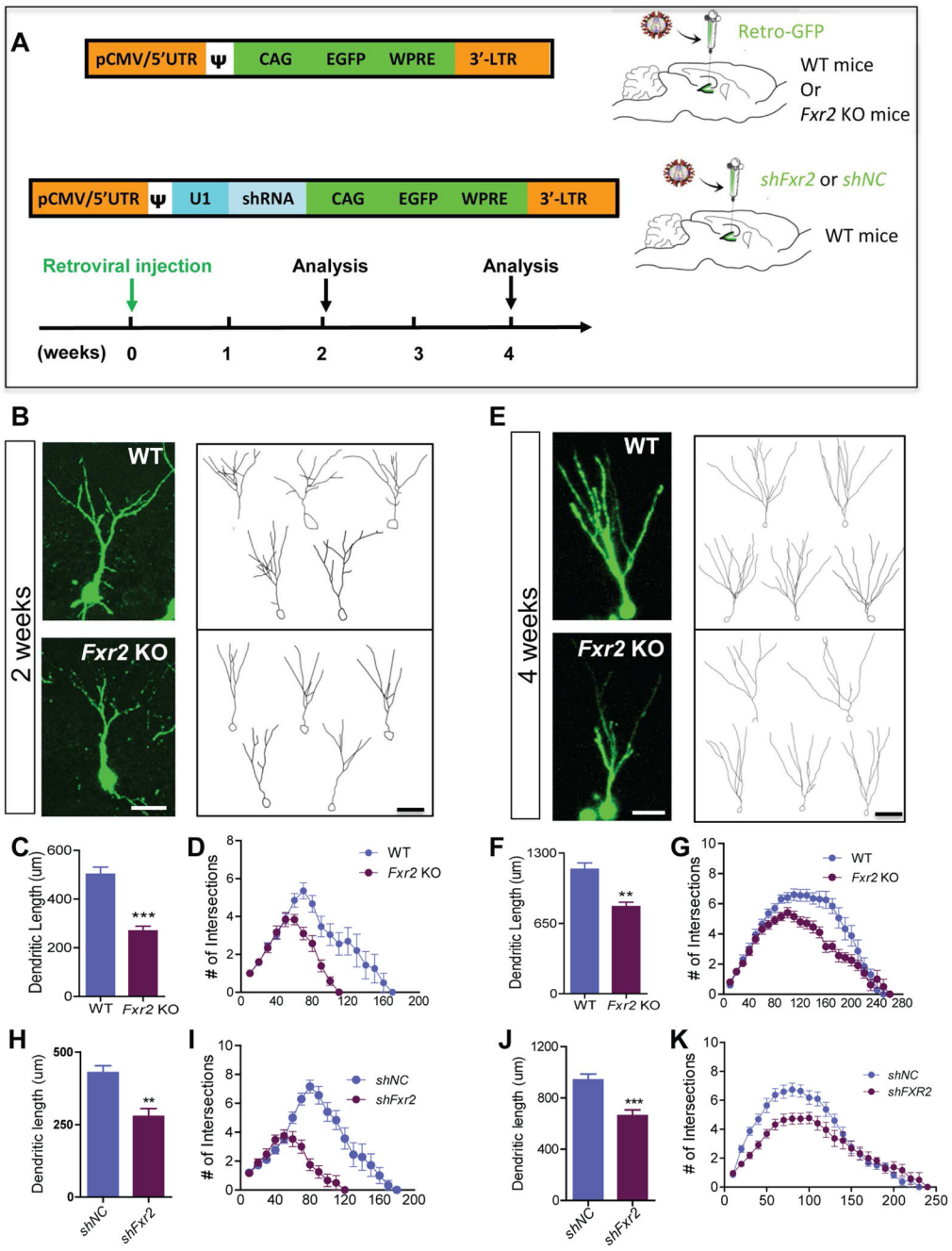

Figure 1. FXR2P Deficiency Leads to Impaired Dendritic Morphogenesis of Newborn Neurons in the Adult Hippocampus

(A) A schematic illustration of the retroviral vectors and the timeline of the experiments for in vivo maturation analyses of newborn neurons in the adult DG. Retroviral vector expressing GFP was used to inject wild-type (WT) and FXR2P mutant (*Fxr2 KO*) mice for B–G. Retroviral vectors expressing either shRNA against FXR2P (*shFxr2*) or control (*shNC*) were used to inject WT mice for H–K.

(B, E) Representative images (left) and sample traces generated by Neurolucida™ (right) of GFP-expressing newborn neurons at 2 weeks post-retrovirus injection (wpi, B) and 4 wpi (E). Scale bars, 50 μm.

(C, D) The dendritic length (C, n = 34 neurons/genotype, $p < 0.0001$) and dendritic complexity (D, $F_{1,64} = 16.5$, $p < 0.001$) of GFP-expressing new DG neurons in *Fxr2* KO and WT mice at 2 wpi.

(F, G) The dendritic length (F, n = 20 neurons/genotype, $p < 0.0001$) and dendritic complexity (G, $F_{1,40} = 8.85$ $p = 0.005$) of GFP-expressing new DG neurons in *Fxr2* KO and WT mice at 4 wpi.

(H–K) The dendritic length (H, 2 wpi, $p = 0.0055$; J, 4 wpi, $p < 0.0001$) and dendritic complexity (I, 2 wpi, $F_{1,40} = 27.56$, $p < 0.001$; K, 4wpi, MANOVA, $F_{1,44} = 13.56$ $p = 0.001$) of GFP-expressing new DG neurons with acute knockdown of FXR2P (retorivurs-*shFxr2)* in the adult newborn neurons compared to controls (*shNC*). (H, I, n = 19 neurons/genotype. J, K, n = 22 neurons/genotype.) See also Figure S1 and Figure S2.

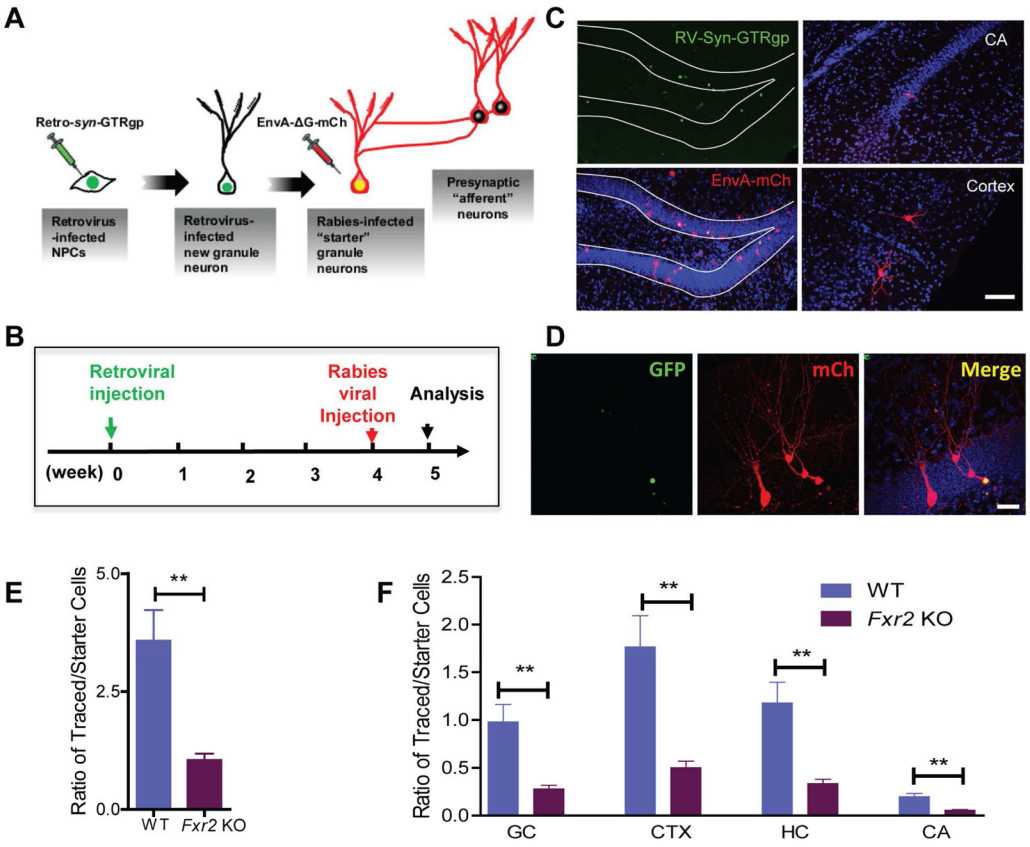

Figure 2. FXR2P Deficiency Leads to Impaired Neural Network Integration of Newborn Neurons

(A) Schematic illustration of pseudo-typed rabies virus-mediated monosynaptic retrograde tracing to map the presynaptic inputs to newborn neurons in the DG. RV-Syn-GTRgp, retrovirus-expressing GFP, TVA, and rabies virus GapPol proteins, driven by a neuronal synapsin promoter. Retrovirus infects only dividing cells, including neural progenitors (NPCs), in the adult DG. EnvA-mCherry, EnvA pseudo-typed rabies virus expressing mCherry can only infect new neurons expressing TVA receptor for EnvA coat protein.

(B) Schematic illustration of timeline of the rabies virus-mediated monosynaptic retrograde tracing experiment.

(C) Sample confocal images showing newborn cells (both green and red) in the DG, and traced cells (red only) in DG, hilus regions, CA regions, and cortex. Scale bar, 200 μm.

(D) High-magnification confocal images of the newborn cells (green and red) and traced cells (red alone) in the DG. Scale bar, 50 μm.

(E, F) The ratio of "Traced Cells (mCh+)" to "Starter Cells" (GFP+mCh+) in total brain (E, n = 5 mice/condition, P = 0.0052; WT: 24 GFP+mCh+ cells/mouse; 85 mCh+ cells/mouse; KO: 27 GFP+mCh+ cells/mouse; 28 mCh+ cells/mouse) or in specific brain regions (F, GC, WT, 24 mCh+ cells/mouse, KO 8 mCh+ cells/mouse, p = 0.0056; cortex cells, CTX, WT, 43 mCh+ cells/mouse, KO, 14 mCh+ cells/mouse, p = 0.005; hilar cells, HC, WT, 29 mCh+ cells/mouse, KO, mCh+ cells/mouse, P = 0.005; and CA cells, WT, 5 mCh+ cells/mouse, KO, 2 mCh+ cells/mouse, p = 0.006) of *Fxr2* KO mice compared to WT mice. **, p <0.01.

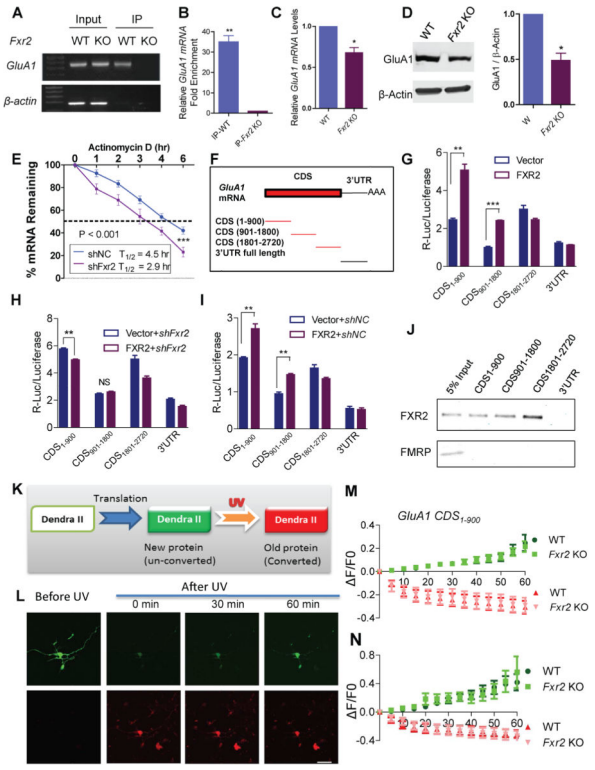

Figure 3. FXR2P Enhances the Stability of *GluA1* mRNA

(A, B) RNA immunoprecipitation (IP) using an anti-FXR2P antibody, followed by PCR (A) or quantitative real-time PCR (B, n = 3, p = 0.0079) analyses of IP RNA showing enrichment of *GluA1* in WT mice, but not in *Fxr2* KO brains. As a negative control, Actin mRNA did not show enrichment in IP RNAs. Input, RNA isolated from samples before IP.

(C) Relative *GluA1* mRNA expression levels in *Fxr2* KO and WT brains determined using real-time PCR. (n = 4, p = 0.0139.)

(D) GluA1 protein expression levels in *Fxr2* KO and WT brains determined by Western blot analyses and quantification. (n = 3, p = 0.0229.)

(E) *GluA1* mRNA stability analyzed in primary hippocampal neurons treated with actinomycin D. The percentage of *GluA1* mRNA was quantified using real-time PCR at the indicated time point. The dotted line indicates 50% of mRNA remaining. Comparisons of the different decay rates were performed by two-way ANOVA: (P = 0.001, n = 3.) Half-life of decay was calculated after transforming data to ln.

(F) Schematic illustration of the coding sequences (CDS) and 3′UTR of *GluA1* mRNA analyzed in G–N.

(G–I) The CDSs and 3′UTR of GluA1 were cloned into a dual luciferase reporter construct to determine the regions of GluA1 mRNA that mediate the regulation of GluA1 protein expression by FXR2P. FXR2P enhances the Renilla luciferase (R-luc) expression (activities, normalized to internal control firefly luciferase activities) through nucleotide 1 to 1800 of the CDS (CDS 1-900 and CDS 901-1800) of GluA1 mRNA sequences (G), which was abolished by acute knockdown of FXR2P (*shFxr2*, H), but not by control shRNA (*shNC*, I). (n = 3.)

(J) Western blot analysis of FXR2P and FMRP proteins in biotin-labeled synthetic *GluA1* mRNA pull-down assays. Input shows 1% of the amount of FXR2P and FMRP in the total lysate used for pull down.

(K) Schematic illustration showing how photoconvertible Dendra II serves as a reporter for real-time protein synthesis and degradation. Upon UV treatment, Dendra II protein converts from green to red fluorescence.

(L) Cultured primary hippocampal neurons were transfected with Dendra II and imaged before and after UV conversion. Scale bar, 50 μm.

(M, N) The green and red fluorescence intensities at the indicated time point after UV conversion were normalized to the starting intensities in the hippocampal neurons transfected with the plasmids expressing DendraII-GluA1 CDS1-900 fusion protein (M, n = 6 neurons/genotype, green fluorescence, $F_{12,120} = 0.18$, $p = 0.99$; red fluorescence, $F_{12,120} = 0.221$, $p = 0.99$) or DenraII-GluA1901-1800 fusion protein (N, n = 6 neurons/genotype, green fluorescence, $F_{12,120} = 0.42$, $p = 0.9533$; red fluorescence, $F_{12,120} = 0.51$, $p = 0.9068$). *, $p < 0.05$; **, $p < 0.01$; ***, $p < 0.001$. See also Figure S3 and Figure S4.

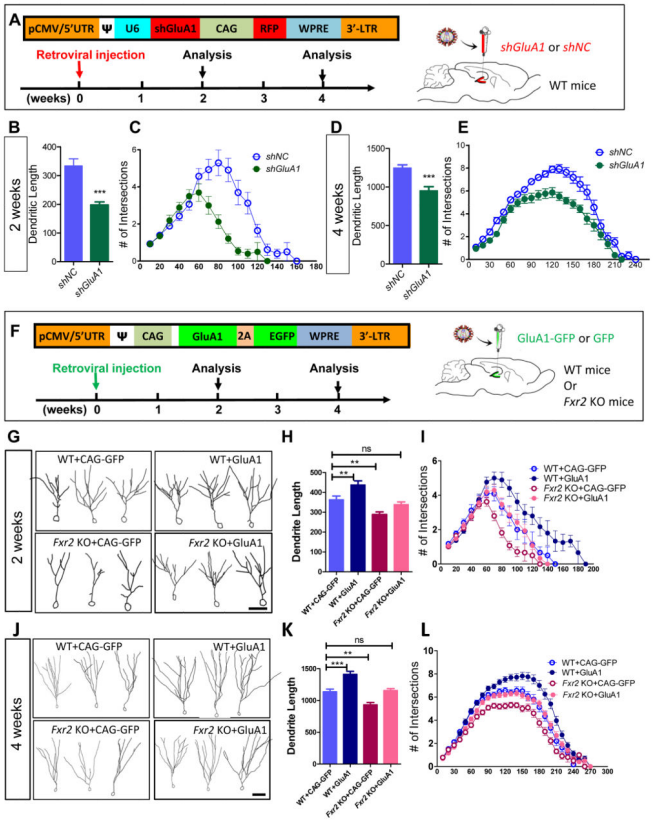

Figure 4. GluA1 Is Important for the Dendritic Development of Newborn Neurons in Adult Hippocampus

(A) A schematic illustration of the retroviral vector expressing shRNA for in vivo acute knockdown of GluA1 expression (*shGluA1*) and the timeline of the experiment.

(B–E) Dendritic length (B, 2 wpi, $p < 0.001$; D, 4 wpi, $p < 0.001$) and dendritic complexity (C, 2 wpi, MANOVA, $F_{1,52} = 8.958$, $p = 0.004$; E, 4 wpi, MANOVA, $F_{1,48} = 21.045$, $p < 0.001$) of RFP-expressing new DG neurons with acute knockdown of GluA1 (*shGluA1)* compared to controls *(shNC)* at 2 and 4 wpi. (B, C, *shNC* n = 21 neurons; *shGluA1*, n = 26 neurons). (D, E, n = 26/condition)

(F) A schematic illustration of the retroviral vector expressing GluA1 and GFP used for in vivo GluA1 rescue.

(G, J) Sample traces generated by Neurolucida™ of retroviral-labeled new neurons in the adult DG at 2 (g) and 4 (j) wpi. Scale bar, 50 μm.

(H, I, K, L) The dendritic length (H, 2 wpi; K, 4 wpi; **, $p < 0.01$; ***,$p < 0.001$; One-Way ANOVA Dunnett's Multiple Comparison post-hoc test with WT+CAG-GFP as the control) and dendritic complexity (I, 2 wpi, WT+CAG-GFP vs. WT+GluA1, MANOVA, $F_{1,70} = 10.822$, $p = 0.002$; *Fxr2* KO+CAG-GFP vs. *Fxr2* KO+GluA, MANOVA, $F_{1,79} = 28.171$ $p < 0.001$; L, 4 wpi, WT+CAG-GFP vs. WT+GluA1, MANOVA, $F_{1,93} = 12.711$, $p = 0.001$; *Fxr2* KO+CAG-GFP vs. *Fxr2* KO+GluA1-, MANOVA, $F_{1,99} = 23.675$, $p < 0.001$) of GFP-expressing new DG neurons in WT and KO mice expressing either GluA1 or control at 2 and 4 wpi. *, $p < 0.05$; **, $p < 0.01$; ***, $p < 0.001$. (n = 46–90 neurons/condition.) See also Figure S5.

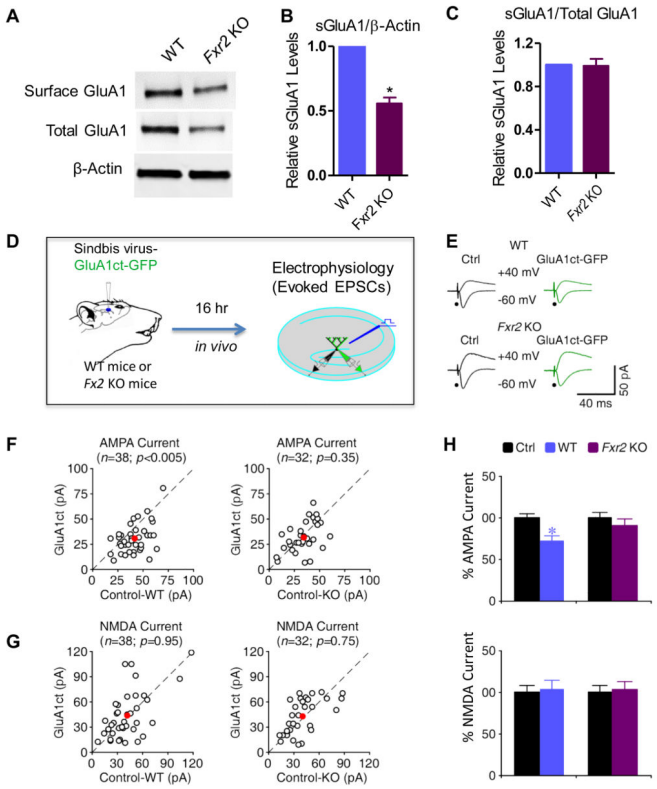

Figure 5. GluA1-Mediated Synaptic AMPA Current Is Reduced in *Fxr2* KO Mice in vivo

(A) Representative western blotting analysis of surface and total GluA1 protein levels in *Fxr2* KO and WT brains.

(B) Quantitative data of relative surface GluA1 protein levels normalized to β-Actin in *Fxr2* KO brains compared to WT brains. (n = 3, p = 0.0104.)

(C) Quantitative data of relative surface GluA1 protein expression normalized to total GluA1 in *Fxr2* KO brains compared to WT brains. (n = 3, p = 0.9055.)

(D) Schematic drawing outlines the in vivo experimental design.

(E) Evoked AMPA-R- (-60 mV) and NMDA-R- (+40 mV) mediated responses recorded from GluA1ct-GFP-expressing and neighboring non-expressing (Ctrl) neurons from WT and *Fxr2* KO mice.

(F–G) Amplitudes of synaptic AMPA and NMDA responses in GluA1ct-GFP-expressing neurons are plotted against those obtained from control non-expressing neurons in WT and *Fxr2* KO mice. Note the red dot (the average value) shifted below the midline in the plot of AMPA responses in WT neurons, suggesting a significant contribution of GluA1-containing AMPA-R-mediated transmission in WT neurons.

(H) Upper, histograms show the relative values of AMPA responses in GluA1ct-GFP-expressing neurons compared to control non-expressing neurons in WT (Ctrl: −43.2 ± 2.1 pA; Exp: −31.3 ± 2.4 pA; n = 38; p <0.005) and *Fxr2* KO (Ctrl: −36.1 ± 2.4 pA; Exp: −32.8 ± 2.7 pA; n = 32; p = 0.35 for *Fxr2* KO) mice. Lower, histograms show the relative values of NMDA responses in GluA1ct-GFP-expressing neurons compared to control non-expressing neurons in WT (Ctrl: 43.8 ± 3.6 pA; Exp: 45.1 ± 4.6 pA; n = 38; p = 0.95) and *Fxr2* KO (Ctrl: 42.3 ± 3.5 pA; Exp: 43.6 ± 3.7 pA; n = 32; p = 0.75 for *Fxr2* KO) mice.

Asterisks indicate $p<0.05$ (Wilcoxon tests). Note the more significantly reduced AMPA responses in GluA1ct-GFP-expressing neurons in WT mice compared to *Fxr2* KO mice ($p<0.05$; Mann-Whitney rank sum tests). See also Figure S6.

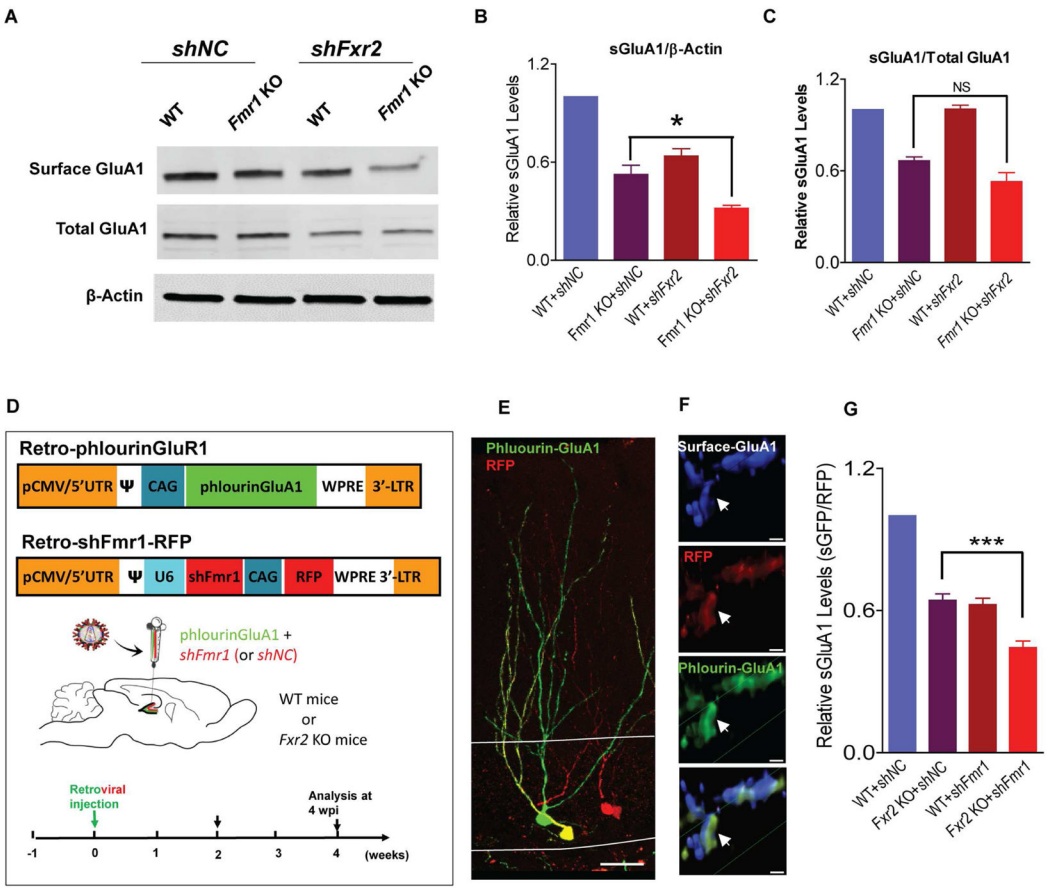

Figure 6. FMRP and FXR2P Synergistically Regulate Surface GluA1 Levels via Distinct Mechanisms

(A–C) Western blot analyses of surface AMPARs in primary cultured neurons showing relative surface GluA1 protein levels normalized to β-Actin (B,, n = 4, WT+*shNC* vs. *Fmr1* KO+*shNC*; p = 0.0001; WT+shNC vs. WT+*shFxr2*, p < 0.001; *Fmr1* KO+*shNC* vs *Fmr1* KO+*shFxr2*, p<0.05; One-Way ANOVA Bonferroni's Multiple Comparison post-hoc test) and relative surface GluA1 protein levels normalized to total GluA1 (C, n = 4, WT+*shNC* vs. *Fmr1* KO+*shNC*; p < 0.001; WT+shNC vs. WT+*shFxr2*, p = 0.88; *Fmr1* KO+*shNC* vs *Fmr1* KO+*shFxr2*, p = 0.08; One-Way ANOVA Bonferroni's Multiple Comparison post-hoc test).

(D) Schematic illustration of retroviral vectors expressing phlourinGluA1 or *shFmr1*-RFP (or *shNC*-RFP) and stereotaxic injection of dual retroviruses.

(E) A representative image of phlourinGluA1- (green) and RFP- (red) labeled newborn neurons in the adult DG. Scale bar, 50 μm.

(F) Super-resolution confocal images of surface phluourinGluA1 expression (blue) in the dendrites and spines of newborn neurons infected with the dual retroviruses (red and green). Scale bar, 5 μm.

(G) Quantitative analyses of relative surface phlourinGluA1 expression normalized to RFP. (n = 10, WT+*shNC* vs. *Fxr2* KO+*shNC*, p < 0.0001; WT+*shNC* vs. WT+*shFmr1*, p< 0.0001;

Fxr2 KO+*shNC* vs *Fxr2* KO+*shFmr1*, p = 0.0017, one-way ANOVA Bonferroni's Multiple Comparison post-hoc test.) *, $p < 0.05$; **, $p < 0.01$; ***, $p < 0.001$.

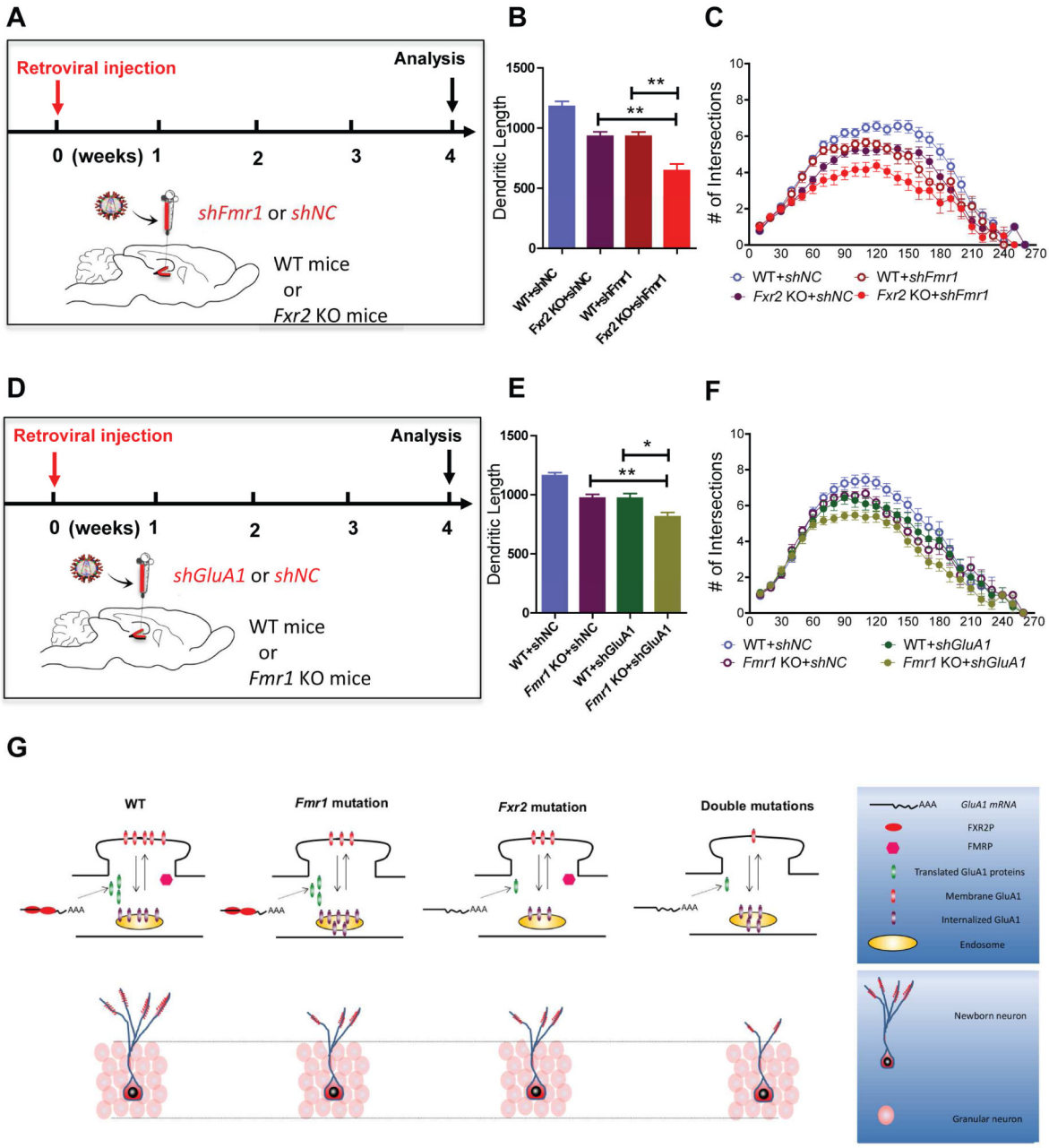

Figure 7. FMRP and FXR2P Additively Regulate the Dendritic Development of Newborn Neurons in the Adult Hippocampus

(A) A schematic illustration of the retroviral vector-expressing shRNA used for in vivo knockdown of FMRP (*shFmr1*) expression either in WT or *Fxr2* KO mice.

(B, C) Quantitative dendritic length (B, *Fxr2 KO+shNC* vs *Fxr2 KO+shFmr1*, $p < 0.01$; *WT +shFmr1* vs *Fxr2 KO+shFmr1*, $p < 0.01$; one-way ANOVA Bonferroni's Multiple Comparison post-hoc test) and dendritic complexity (C, MANOVA, $F_{2,90} = 7.564$, $p = 0.001$, n = 21–67 neurons/condition,) of RFP-expressing new DG neurons in WT and *Fxr2* KO mice expressing either *shFmr1* or *shNC* at 4 wpi.

(D) A schematic illustration of the retroviral vector-expressing shRNA used for in vivo knockdown of GluA1 expression (*shGluA1*) either in WT or *Fmr1* KO mice.
(E, F) Quantitative dendritic length (E, *Fmr1 KO+shNC* vs *Fmr1 KO+shGluA1*, $p < 0.01$; *WT+shGluA1* vs *Fmr1 KO+shGluA1*, $p < 0.05$; one-way ANOVA Bonferroni's Multiple Comparison post-hoc test) and dendritic complexity (F, MANOVA, $F_{2,71} = 5.026$, $p = 0.009$, n = 22 neurons/condition) of RFP-expressing new DG neurons in WT and *Fmr1* KO mice expressing either *GluA1* shRNA and control at 4 weeks after retrovirus-mediated gene transduction.
(G) Model of FMRP and FXR2P regulation of GluA1 membrane levels and dendritic development of newborn neurons in the adult DG. *, $p < 0.05$; **, $p < 0.01$; ***, $p < 0.001$. See also Figure S7.